

Extended stochastic block models

Sirio Legramanti¹, Tommaso Rigon², Daniele Durante³, David B. Dunson²

Abstract

Stochastic block models (SBM) are widely used in network science due to their interpretable structure that allows inference on groups of nodes having common connectivity patterns. Although providing a well established model-based approach for community detection, such formulations are still the object of intense research to address the key problem of inferring the unknown number of communities. This has motivated the development of several probabilistic mechanisms to characterize the node partition process, covering solutions with fixed, random and infinite number of communities. In this article we provide a unified view of all these formulations within a single extended stochastic block model (ESBM), that relies on Gibbs-type processes and encompasses most existing representations as special cases. Connections with Bayesian nonparametric literature open up new avenues that allow the natural inclusion of several unexplored options to model the nodes partition process and to incorporate node attributes in a principled manner. Among these new alternatives, we focus on the Gnedin process as an example of a probabilistic mechanism with desirable theoretical properties and nice empirical performance. A collapsed Gibbs sampler that can be applied to the whole ESBM class is proposed, and refined methods for estimation, uncertainty quantification and model assessment are outlined. The performance of ESBM is assessed in simulations and an application to bill co-sponsorship networks in the Italian parliament, where we find key hidden block structures and core-periphery patterns.

Keywords

Bayesian nonparametric — community detection — Gibbs-type prior — network data — product partition model

¹Department of Decision Sciences. Bocconi University, via Röntgen 1, 20136, Milan, Italy

²Department of Statistical Science, Duke University, Box 90251, Durham, North Carolina 27708, U.S.A.

²Department of Decision Sciences and Bocconi Institute for Data Science and Analytics. Bocconi University, via Röntgen 1, 20136, Milan, Italy

Contents

1	Introduction	1
2	Model Formulation	2
2.1	Stochastic Block Models	2
2.2	Extended Stochastic Block Model	3
	Learning the number of communities • Asymptotic properties • Inclusion of node attributes	
3	Posterior computations and inference	5
3.1	Collapsed Gibbs Sampler	5
3.2	Estimation, uncertainty quantification, inference .	6
4	Simulation Studies	7
5	Bill co-sponsorship networks	8
6	Discussion	9
	References	9

1. Introduction

Network data are ubiquitous in science and there is recurring interest in community structure. Interacting units—such as brain regions [7], genes [29], social actors [50] and transportation nodes [19]—can often be grouped into clusters which share similar connectivity patterns in the corresponding network. The relevance of such a property and the interdisci-

plinary nature of network science have motivated a collective effort by various disciplines towards the development of methods for community detection, ranging from algorithmic strategies [16, 36, 34, 4, 42] to model-based solutions [22, 38, 25, 1, 2, 15]; see also [10, 26] for a comprehensive overview. Despite being widely used in practice, most algorithmic approaches lack uncertainty quantification and can only detect communities characterized by dense within-block connectivity and sparser connections between different blocks [11]. These issues have motivated a growing interest in model-based solutions which rely on generative statistical models. This choice allows coherent uncertainty quantification, model selection and hypothesis testing, while accounting for more general connectivity patterns, where nodes in the same community are not necessarily more densely connected, but simply share the same connectivity behavior [11], which may even characterize core-periphery, disassortative or weak community patterns [11] [Figure 8]. These alternative structures are also found in the motivating 2013–2018 Italian bill co-sponsorship network [5] displayed in Figure 1, thus supporting our focus on model-based solutions.

Among the generative models for learning communities in network data, the stochastic block model (SBM) [22, 38] is arguably the most widely implemented and well-established formulation, owing also to its unique balance between sim-

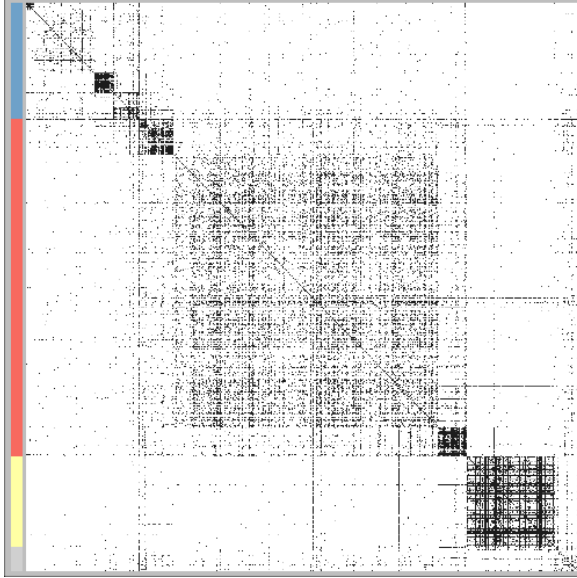


Figure 1. Adjacency matrix of the 2013–2018 bill co-sponsorship network in the Italian parliament. Edges and non-edges are depicted as black and white pixels, respectively. Colors on the left denote the right wing (blue), left wing (red), *Movimento 5 Stelle* (yellow) and mixed group (grey).

plicity and flexibility [26]. In SBMs, the probability of an edge between two nodes only depends on their cluster memberships, thus allowing efficient inference on communities and on block probabilities—which can characterize assortative, disassortative, core–periphery or weak community patterns, and combinations of such structures [11]. These desirable properties have motivated extensive theoretical studies [51, 3, 39] and various generalizations [48, 25, 20, 1, 23, 45, 35, 15, 12, 47] of the original SBM.

Most of the above extensions aim at addressing two fundamental open problems with classical SBMs. First, in real-world applications the number of underlying communities is typically unknown and has to be learned from the data. Therefore, classical SBM formulations based on a fixed and pre-specified number of communities [22, 38] are not suitable to address this goal. Second, it is common to observe nodal attributes that may effectively inform the community assignment mechanism. Hence, SBMs require extensions to include such information in the process regulating the node partitions. A successful answer to the first open issue has been provided by Bayesian nonparametric solutions replacing the original Dirichlet–multinomial process for node partitioning [38] with alternative priors that allow the number of communities to grow adaptively with the size of the network via the Chinese restaurant process (CRP) [25, 45] or be finite and random under a mixture of finite mixtures representation [15]. Inclusion of nodal attributes within the community assignment is instead obtained via multinomial probit [48] or mixture models [35, 47]. Unfortunately, all these different extensions have been developed separately and SBMs still lack a unifying framework, which would be useful to clarify common properties, develop broad computational and inferential strategies, and identify novel solutions.

Motivated by the above discussion, we unify the aforementioned formulations within a general extended stochastic block model (ESBM) framework based on Gibbs-type priors [18, 8], which also allow the inclusion of node attributes in a principled manner via product partition models (PPMs) [21]. Within this class, we focus on the Gneden process [17] as an example of a prior which has not yet been employed in the context of SBMs, but exhibits analytical tractability, desirable properties, theoretical guarantees and promising empirical performance when combined with such models. Our framework allows posterior computation via an easy-to-implement collapsed Gibbs sampler, and motivates general methods for uncertainty quantification and model assessment, thus exploiting the advantages of a model-based approach over algorithmic strategies. The performance of key priors within the ESBM class is evaluated in simulations. In light of these results, we opt for the Gneden process to analyze the political network in Figure 1. Code and data are available at <https://github.com/danieledurante/ESBM>, where we also provide additional figures and empirical analyses.

2. Model Formulation

Consider a binary undirected network with V nodes and let \mathbf{Y} denote its $V \times V$ symmetric adjacency matrix, with elements $y_{vu} = y_{uv} = 1$ if nodes v and u are connected, and $y_{vu} = y_{uv} = 0$ otherwise. Since the focus is on community detection, self-loops are not relevant and, hence, are not included in the generative model. We first review SBMs and then introduce our general ESBM class along with associated properties and extensions to incorporate node attributes. For simplicity, we focus on binary undirected networks and categorical attributes, but our approach can be naturally extended to other types of networks and covariates, as highlighted in the final discussion.

2.1 Stochastic Block Models

SBMs [22, 38] partition the nodes into \bar{H} mutually exclusive and exhaustive communities, with nodes in the same community sharing common connectivity patterns. More specifically, SBMs assume the sub-diagonal entries y_{vu} , $v = 2, \dots, V$, $u = 1, \dots, v-1$ of the symmetric adjacency matrix \mathbf{Y} are conditionally independent Bernoulli random variables with probabilities depending only on the community memberships of the involved nodes v and u . Denoting with $\bar{\mathbf{z}} = (\bar{z}_1, \dots, \bar{z}_V)^\top \in \{1, \dots, \bar{H}\}^V$ the vector of community assignments of the V nodes, and with Θ the $\bar{H} \times \bar{H}$ symmetric matrix whose generic element θ_{hk} is the probability of a connection between a node in community h and a node in community k , the likelihood for the adjacency matrix \mathbf{Y} is

$$\begin{aligned} p(\mathbf{Y} | \bar{\mathbf{z}}, \Theta) &= \prod_{v=2}^V \prod_{u=1}^{v-1} \theta_{\bar{z}_v \bar{z}_u}^{y_{vu}} (1 - \theta_{\bar{z}_v \bar{z}_u})^{1-y_{vu}} \\ &= \prod_{h=1}^{\bar{H}} \prod_{k=1}^h \theta_{hk}^{m_{hk}} (1 - \theta_{hk})^{\bar{m}_{hk}}, \end{aligned} \quad (1)$$

where m_{hk} and \bar{m}_{hk} denote the number of edges and non-edges between communities h and k , respectively. Classical SBMs [22, 38] assume independent Beta(a, b) priors for the block

probabilities θ_{hk} . Thus the joint density for the diagonal and sub-diagonal elements of the symmetric matrix Θ is

$$p(\Theta) = \prod_{h=1}^{\bar{H}} \prod_{k=1}^h \frac{\theta_{hk}^{a-1} (1 - \theta_{hk})^{b-1}}{B(a, b)}, \quad (2)$$

where $B(\cdot, \cdot)$ is the Beta function. Although quantifying prior uncertainty in the block probabilities via (2) is important, the overarching goal in SBMs is to provide inference on communities. Consistent with this focus, Θ is usually treated as a nuisance parameter and marginalized out in (1) via beta-binomial conjugacy, obtaining

$$p(\mathbf{Y} | \bar{\mathbf{z}}) = \prod_{h=1}^{\bar{H}} \prod_{k=1}^h \frac{B(a + m_{hk}, b + \bar{m}_{hk})}{B(a, b)}. \quad (3)$$

As we will clarify in the following sections, such a collapsed representation is also useful for computation and inference. (3) provides a simple likelihood common to several extensions of SBMs, which instead differ in the choice of the probabilistic mechanism underlying the assignments $\bar{\mathbf{z}}$. A natural choice is a Dirichlet–multinomial distribution on $\bar{\mathbf{z}}$, obtained by marginalizing the vector of community assignment probabilities $\pi = (\pi_1, \dots, \pi_{\bar{H}}) \sim \text{Dirichlet}(\beta)$ out of the likelihood for $\bar{\mathbf{z}}$, assuming $\text{pr}(\bar{z}_v = h | \pi) = \pi_h$, $v = 1, \dots, V$. If \bar{H} is fixed and finite, this leads to the original SBM [38]. However, as already discussed, the number of communities is usually unknown and has to be inferred from the data. A possible solution consists in placing a prior on \bar{H} , which leads to the mixture of finite mixtures (MFM) version of the SBM proposed by [15]. Another option is a Dirichlet process partition mechanism, which corresponds to the infinite relational model [25]. Such an infinite mixture model differs from MFM in that $\bar{H} = \infty$, meaning that infinitely many nodes would give rise to infinitely many communities. Note that the total number of possible clusters \bar{H} should not be confused with the number of occupied clusters H . The latter is defined as the number of distinct labels in $\bar{\mathbf{z}}$, and is upper bounded by $\min\{V, \bar{H}\}$. Hence H cannot exceed V , even when $\bar{H} = \infty$.

So far we have introduced *labeled* clusters, identified by $\bar{\mathbf{z}}$. This means that a vector $\bar{\mathbf{z}}$ and its relabelings are regarded as distinct objects, even though they identify the same partition. Throughout the rest of the paper we will rely on a generic \mathbf{z} to denote all relabelings of $\bar{\mathbf{z}}$ that lead to the same partition. For convenience, one may assume that $z_v \in \{1, \dots, H\}$, which corresponds to avoiding empty communities. Note that (3) is invariant under relabeling and, hence, $p(\mathbf{Y} | \mathbf{z}) = p(\mathbf{Y} | \bar{\mathbf{z}})$.

2.2 Extended Stochastic Block Model

As illustrated in the previous section, several priors for community memberships have been considered in the context of SBMs, including the Dirichlet–multinomial [38], the Dirichlet process [25], and mixtures of finite Dirichlet mixtures [15]. These are all Gibbs–type priors, which were introduced by [18] and stand out for analytical and computational tractability [8]. In this section we propose the ESBM as a unifying framework characterized by the choice of a Gibbs–type prior

for the assignments. This formulation includes the previously-mentioned SBMs as special cases and offers new alternatives by exploring the whole Gibbs–type class and its connections with PPMs [21].

Gibbs–type priors are defined over the space of the unlabeled community indicators \mathbf{z} . For $a > 0$, denote the ascending factorial with $(a)_n = a(a+1) \cdots (a+n-1)$ for any $n \geq 1$, and set $(a)_0 = 1$. A probability mass function $p(\mathbf{z})$ is of Gibbs–type if and only if it has the form

$$p(\mathbf{z}) = \mathcal{W}_{V,H} \prod_{h=1}^H (1 - \sigma)_{n_h-1}, \quad (4)$$

where n_h denotes the number of nodes in cluster h , $\sigma < 1$ is a so–called *discount parameter* and $\{\mathcal{W}_{V,H} : 1 \leq H \leq V\}$ is a collection of non–negative weights satisfying the recursion $\mathcal{W}_{V,H} = (V - H\sigma)\mathcal{W}_{V+1,H} + \mathcal{W}_{V+1,H+1}$, with $\mathcal{W}_{1,1} = 1$. Gibbs–type priors are a special case of PPMs [21, 43], which are probability models for random partitions \mathbf{z} of the form $p(\mathbf{z}) \propto c(Z_1) \cdots c(Z_H)$, where $\{Z_1, \dots, Z_H\}$ is the partition associated to \mathbf{z} , so that $v \in Z_h$ if and only if $z_v = h$, whereas $c(\cdot)$ is a non–negative *cohesion function* measuring the homogeneity within each cluster. Such a connection will be useful to incorporate node–specific attributes effects in ESBMs. Interestingly, Gibbs–type priors represent the largest class of PPMs which are also species sampling models [41], meaning that the membership indicators \mathbf{z} can be obtained in a sequential and interpretable manner. Specifically, a Gibbs–type random partition \mathbf{z} can be sequentially generated according to

$$\text{pr}(z_{V+1} = h | \mathbf{z}) \propto \begin{cases} \mathcal{W}_{V+1,H}(n_h - \sigma) & \text{for } h = 1, \dots, H, \\ \mathcal{W}_{V+1,H+1} & \text{for } h = H + 1. \end{cases} \quad (5)$$

Hence, the community assignment process can be interpreted as a simple seating mechanism in which a new node is assigned to an existing community h with probability proportional to the current size n_h of that community discounted by a global factor σ and further rescaled by a weight $\mathcal{W}_{V+1,H}$, which may depend both on the size of the network and on the current number of non–empty communities. Alternatively, the incoming node is assigned to a new community with probability proportional to $\mathcal{W}_{V+1,H+1}$. According to (5), when $\sigma > 0$ the mass assigned to existing communities is less than proportional to their cardinality, particularly affecting small clusters, and the remaining mass is added to the probability of creating a new community. This gives an intuition for why the number of occupied clusters grows with V as $\mathcal{O}(V^\sigma)$ when $\sigma > 0$. When $\sigma = 0$ the growth is slower, namely $\mathcal{O}(\log V)$, while $\sigma < 0$ yields a finite \bar{H} even for infinitely many nodes. This is due to the fact that the reinforcement mechanism is reversed and each new community decreases the probability of creating future ones [8]. In the examples below we show how commonly used partition processes in SBMs and unexplored alternatives can be obtained as special cases of (5).

Example 1 (Dirichlet–multinomial – DM). *Let $\sigma < 0$ and define $\mathcal{W}_{V,H} = \beta^{H-1} / (\beta\bar{H} + 1)_{V-1} \prod_{h=1}^{H-1} (\bar{H} - h) I(H \leq \bar{H})$*

	\bar{H}	σ	H (growth)	Example
I	Fixed	$\sigma < 0$	—	Dirichlet–multinomial (DM)
II	Random	$\sigma < 0$	—	Gnedin process (GN)
III.a	Infinite	$\sigma = 0$	$\mathcal{O}(\log V)$	Dirichlet process (DP)
III.b	Infinite	$\sigma \in (0, 1)$	$\mathcal{O}(V^\sigma)$	Pitman–Yor process (PY)

Table 1. A classification of Gibbs–type priors.

for some $\beta = -\sigma$ and $\bar{H} \in \{1, 2, \dots\}$. Then (5) coincides with the Dirichlet–multinomial urn–scheme

$$\text{pr}(z_{V+1} = h \mid \mathbf{z}) \propto \begin{cases} n_h + \beta & \text{for } h = 1, \dots, H, \\ \beta(\bar{H} - H)I(H \leq \bar{H}) & \text{for } h = H + 1. \end{cases}$$

Example 2 (Dirichlet process – DP). Let $\sigma = 0$ and $\mathcal{W}_{V,H} = \alpha^H / (\alpha)_V$ for some $\alpha > 0$. Then (5) leads to a CRP scheme

$$\text{pr}(z_{V+1} = h \mid \mathbf{z}) \propto \begin{cases} n_h & \text{for } h = 1, \dots, H, \\ \alpha & \text{for } h = H + 1. \end{cases}$$

The CRP can also be obtained as a limiting case of a Dirichlet–multinomial process with $\beta = \alpha/\bar{H}$, as $\bar{H} \rightarrow \infty$.

Example 3 (Pitman–Yor process – PY). Let $\sigma \in [0, 1)$ and set $\mathcal{W}_{V,H} = \prod_{h=1}^{H-1} (\alpha + h\sigma) / (\alpha + 1)_V$ for some $\alpha > -\sigma$. Then (5) characterizes the Pitman–Yor process

$$\text{pr}(z_{V+1} = h \mid \mathbf{z}) \propto \begin{cases} n_h - \sigma & \text{for } h = 1, \dots, H, \\ \alpha + H\sigma & \text{for } h = H + 1. \end{cases}$$

This scheme clearly reduces to the DP when $\sigma = 0$.

Example 4 (Gnedin process – GN). Let $\sigma = -1$ and $\mathcal{W}_{V,H} = (\gamma)_{V-H} \prod_{h=1}^{H-1} (h^2 - \gamma h) / \prod_{v=1}^{V-1} (v^2 + \gamma v)$ for some $\gamma \in (0, 1)$. Then (5) identifies the Gnedin process

$$\text{pr}(z_{V+1} = h \mid \mathbf{z}) \propto \begin{cases} (n_h + 1)(V - H + \gamma) & \text{for } h = 1, \dots, H, \\ H^2 - H\gamma & \text{for } h = H + 1. \end{cases}$$

Other known and popular examples of tractable Gibbs–type priors can be found in [28, 8, 9, 32].

2.2.1 Learning the number of communities

A key focus in community detection is inferring the number of occupied clusters H . As the number of nodes V grows, H converges to \bar{H} , which can be assumed, depending on the application, to be finite (scenario I), random but almost surely finite (scenario II), or infinite (scenario III). Classical SBMs [38] fall into scenario I, the MFM approach of [15] into scenario II, and the infinite relational model of [25] into scenario III. As shown in Table 1, Gibbs–type priors cover all the aforementioned scenarios, allowing analysts to choose the most suitable for a given study.

The only Gibbs–type prior within scenario I is the Dirichlet–multinomial, which serves as a building block for Gibbs–type priors in scenario II. In fact, the latter can be derived from the Dirichlet–multinomial by placing a prior on \bar{H} , thus making

it random. For instance, the distribution $p_G(\mathbf{z}; \gamma)$ of \mathbf{z} under the Gnedin process in Example 4 can be easily expressed as

$$p_G(\mathbf{z}; \gamma) = \sum_{h=1}^{\infty} \text{pr}(\bar{H} = h) p_{\text{DM}}(\mathbf{z}; 1, h),$$

where $p_{\text{DM}}(\mathbf{z}; \beta, \bar{H})$ denotes the Dirichlet–multinomial distribution in Example 1, and $\text{pr}(\bar{H} = h) = \gamma(1 - \gamma)_{h-1} / h!$ can be interpreted as a prior distribution on \bar{H} . Although different prior choices for \bar{H} might be considered [32], the Gnedin process has considerable advantages. Firstly, the sequential mechanism described in Example 4 has a simple analytical expression. Moreover, the distribution $\text{pr}(\bar{H} = h) = \gamma(1 - \gamma)_{h-1} / h!$ has the mode at 1, heavy tail and infinite expectation [17]. Hence, the associated MFM favors simpler models with fewer communities while being also a robust specification for \bar{H} due to the heavy-tailed prior distribution.

Priors on \bar{H} quantify uncertainty in the total number of communities that one would expect if $V \rightarrow \infty$. In practice, the number of non–empty communities H occupied by the observed V nodes is of more direct interest. Under Gibbs–type priors such a quantity has a closed form probability mass function [18] that coincides with

$$\text{pr}(H = h) = \frac{\mathcal{W}_{V,h}}{\sigma^h} \mathcal{C}(V, h; \sigma), \quad h = 1, \dots, V, \quad (6)$$

where $\mathcal{C}(V, h; \sigma) = 1/h! \sum_{j=0}^h (-1)^j j! \{j!(h-j)!\}^{-1} (-j\sigma)_V$ is the generalized factorial coefficient. The CRP is recovered when $\sigma \rightarrow 0$. In <https://github.com/danieledurante/ESBM> we provide code to evaluate such quantities under the Gibbs–type priors in Examples 1–4, and then leverage these values to compute the prior expectation of H —which can assist in choosing the hyperparameters. In our implementation the coefficients $\mathcal{C}(V, h; \sigma)$ were not computed from their definition, but leveraging numerically stable recursive formulas.

In addition to its practical relevance, (6) clarifies the asymptotic behavior of H . Indeed, the distribution of H converges to a point mass in scenario I, to a proper distribution in scenario II and to a point mass at infinity in scenario III. For instance, recalling again the Gnedin process in Example 4, we have that (6) reduces to

$$\text{pr}_G(H = h) = \binom{V}{h} \frac{(1 - \gamma)_{h-1} (\gamma)_{V-h}}{(1 + \gamma)_{V-1}}, \quad h = 1, \dots, V,$$

and hence the expected value can be easily computed as

$$\mathbb{E}(H) = \sum_{h=1}^V h \cdot \binom{V}{h} \frac{(1 - \gamma)_{h-1} (\gamma)_{V-h}}{(1 + \gamma)_{V-1}}.$$

Note that $\lim_{V \rightarrow \infty} \text{pr}(H = h) = \text{pr}(\bar{H} = h) = \gamma(1 - \gamma)_{h-1} / h!$.

2.2.2 Asymptotic properties

Dirichlet and Pitman–Yor processes may lead to inconsistent estimates for the number of communities if the data are generated from a model with $\bar{H}_0 < \infty$ [31]. Intuitively, priors in scenario III fail in estimating a finite \bar{H}_0 because, by assumption, $\bar{H} = \infty$. Hence, we suggest Gibbs–type priors with $\sigma \geq 0$ only if the analyst believes that $\bar{H}_0 = \infty$, that is, when the true number of communities is assumed to grow without bound with the number of nodes V .

If the analyst believes that $\bar{H}_0 < \infty$, then Gibbs–type priors of scenario II may be more suitable. In the context of SBMs, [15] proved a consistency result for a MFM, that actually applies to any Dirichlet–multinomial with a prior on \bar{H} supported on all positive integers. For instance, consistency holds for the Gneden process in Example 4.

2.2.3 Inclusion of node attributes

When node–specific attributes $\mathbf{x}_v = (x_{v1}, \dots, x_{vd})^\top$, $v = 1, \dots, V$ are available, such information may support inference on community structures, both in term of point estimation and in reduction of posterior uncertainty. An option to include attributes within ESBMs in a principled manner is to rely on the PPM structure of Gibbs–type priors. Adapting results in [40, 33] to our network setting, this solution is based on the idea of replacing (4) with

$$p(\mathbf{z} \mid \mathbf{X}) \propto \mathcal{W}_{V,H} \prod_{h=1}^H p(\mathbf{X}_h) (1 - \sigma)_{n_h-1}, \quad (7)$$

where $\mathbf{X} = (\mathbf{x}_1, \dots, \mathbf{x}_V)^\top$, whereas $\mathbf{X}_h = (\mathbf{x}_v : z_v = h)$ are the attributes for the nodes in cluster h . In (7), $p(\mathbf{X}_h)$ controls the contribution of the attributes to the cluster cohesion and, as we will clarify later, it favors communities that are homogeneous with respect to attribute values. Even if attributes are not considered random, in this context [33] suggests choosing $p(\mathbf{X}_h)$ as the probability distribution induced by an auxiliary model $p(\mathbf{X}_h \mid \xi_h)$, with ξ_h denoting community–specific parameters, thus obtaining $p(\mathbf{X}_h) = \int p(\mathbf{X}_h \mid \xi_h) d\xi_h$. We refer to [33] for further discussion about the choice of $p(\cdot)$.

In this work, we consider the case in which each node attribute $\mathbf{x}_v = x_v$ is a single categorical variable taking values in $\{1, \dots, C\}$. This is a common setting in applications, where node attributes often come in the form of exogenous partitions. For example, in the Italian bill co–sponsorship network in Figure 1, possible attributes are party or coalition memberships, that we expect to influence voting behaviors. Following [33], we consider a Dirichlet–multinomial auxiliary model for such attributes, which leads to

$$p(\mathbf{X}_h) \propto \frac{1}{\Gamma(n_h + \alpha_0)} \prod_{c=1}^C \Gamma(n_{hc} + \alpha_c), \quad (8)$$

where n_{hc} is the number of nodes in cluster h with attribute value c , and $\alpha_0 = \sum_{c=1}^C \alpha_c$, with $\alpha_c > 0$ for $c = 1, \dots, C$.

3. Posterior computations and inference

We derive a collapsed Gibbs sampler that holds for any model within the ESBM class, and allows inclusion of node attributes.

Then, we provide extensive tools not only for point estimation of the community structure, but also for uncertainty quantification and model selection. Despite their importance, these two aspects have been largely neglected in the SBM literature.

3.1 Collapsed Gibbs Sampler

The availability of the urn scheme in (5) for the whole class of Gibbs–type priors allows us to derive a collapsed Gibbs sampler that holds for any ESBM (see Algorithm 1). At each iteration, we sample the community assignment of each node v from its full–conditional distribution given the adjacency matrix \mathbf{Y} and the vector \mathbf{z}_{-v} of the cluster assignments of all the other nodes. By simple application of the Bayes rule, these full conditional probabilities are equal to

$$\text{pr}(z_v = h \mid \mathbf{Y}, \mathbf{z}_{-v}) = \text{pr}(z_v = h \mid \mathbf{z}_{-v}) \frac{p(\mathbf{Y} \mid z_v = h, \mathbf{z}_{-v})}{p(\mathbf{Y} \mid \mathbf{z}_{-v})}. \quad (9)$$

Recalling [45], the last term in (9) simplifies to

$$\prod_{k=1}^H \frac{\text{B}(a + m_{hk}^- + r_{vk}, b + \bar{m}_{hk}^- + n_k^- - r_{vk})}{\text{B}(a + m_{hk}^-, b + \bar{m}_{hk}^-)}, \quad (10)$$

where m_{hk}^- and \bar{m}_{hk}^- denote the number of edges and non–edges between clusters h and k , without counting node v , and r_{vk} is the number of edges between node v and the nodes in cluster k . The prior term $\text{pr}(z_v = h \mid \mathbf{z}_{-v})$ in (9) is derived from (5) and coincides with

$$\text{pr}(z_v = h \mid \mathbf{z}_{-v}) \propto \begin{cases} \mathcal{W}_{V,H^-}(n_h^- - \sigma) & \text{for } h \leq H^-, \\ \mathcal{W}_{V,H^-+1} & \text{for } h = H^- + 1, \end{cases} \quad (11)$$

where n_h^- and H^- are the cardinality of cluster h and the number of occupied communities, respectively, after removing node v from \mathbf{Y} . Under the priors in Table 1, (11) admits the simple closed–form expressions reported in Examples 1–4.

When available, nodal attributes can be incorporated via (7), leading to an attribute–dependent collapsed Gibbs sampler. In this case, the full conditionals in (9) become

$$\text{pr}(z_v = h \mid \mathbf{Y}, \mathbf{X}, \mathbf{z}_{-v}) \propto \text{pr}(z_v = h \mid \mathbf{Y}, \mathbf{z}_{-v}) \frac{p(\mathbf{X}_h)}{p(\mathbf{X}_{h,-v})}, \quad (12)$$

where \mathbf{X}_h and $\mathbf{X}_{h,-v}$ are the attributes for the nodes in the h th community, including and excluding node v , respectively. In the case of categorical attributes with $p(\mathbf{X}_h)$ as in (8), the last term in (12) can be written as

$$\frac{p(\mathbf{X}_h)}{p(\mathbf{X}_{h,-v})} = \frac{n_{hx_v}^- + \alpha_{x_v}}{n_h^- + \alpha_0}, \quad (13)$$

where n_{hc} is the number of nodes in cluster h with covariate value c and n_h^- is the total number of nodes in cluster h , both without counting node v . The introduction of this additional term favors the attribution of node v to the cluster(s) containing a higher fraction of nodes with its same covariate value x_v . In fact, (13) tends to the fraction of nodes in cluster h that have the same attribute value as node v . Instead, for $h = H^- + 1$ the additional term is equal to α_{x_v}/α_0 .

Algorithm 1: Gibbs sampler for ESBM

At each iteration, update the cluster assignments as follows:

For $v = 1, \dots, V$ **do**:

1. Remove node v from the network;
2. If the cluster which contained node v contains no other node, discard it (so that clusters $1, \dots, H^-$ are non-empty);
3. Sample z_v from a categorical distribution with probabilities

$$\text{pr}(z_v = h \mid \mathbf{Y}, \mathbf{z}_{-v}) = \text{pr}(z_v = h \mid \mathbf{z}_{-v}) \cdot \frac{p(\mathbf{Y} \mid z_v = h, \mathbf{z}_{-v})}{p(\mathbf{Y} \mid \mathbf{z}_{-v})},$$

for $h = 1, \dots, H^- + 1$, with $\text{pr}(z_v = h \mid \mathbf{z}_{-v})$ as in (11) and $p(\mathbf{Y} \mid z_v = h, \mathbf{z}_{-v})/p(\mathbf{Y} \mid \mathbf{z}_{-v})$ as in (10). If categorical node attributes are available and have to be incorporated via (7)–(8), rescale the above expression by (13).

Finally, although Algorithm 1 leverages the marginal likelihood in (3) with block probabilities integrated out, estimates for each θ_{hk} can be easily obtained. In particular, since $(\theta_{hk} \mid \mathbf{Y}, \mathbf{z}) \sim \text{Beta}(a + m_{hk}, b + \bar{m}_{hk})$, we estimate θ_{hk} by

$$\hat{\theta}_{hk} = \mathbb{E}[\theta_{hk} \mid \mathbf{Y}, \mathbf{z} = \hat{\mathbf{z}}] = \frac{a + \hat{m}_{hk}}{a + \hat{m}_{hk} + b + \hat{\bar{m}}_{hk}}, \quad (14)$$

where \hat{m}_{hk} and $\hat{\bar{m}}_{hk}$ denote the number of edges and non-edges between nodes in communities h and k computed from the estimated cluster assignment $\hat{\mathbf{z}}$. In the next subsection, we describe methods for estimation of \mathbf{z} , uncertainty quantification in community detection, and model selection.

3.2 Estimation, uncertainty quantification, inference
 While algorithmic methods return a single estimated partition, ESBMs provide the whole posterior distribution over the space of partitions. To fully exploit such a posterior, we adapt the decision-theoretic approach of [49] to the community detection setting. In this way, we summarize posterior distributions on partitions leveraging the *variation of information* (VI) metric [30], which quantifies distances between two clusterings by comparing their individual and joint entropies, and ranges from 0 to $\log_2 V$. Intuitively, VI measures the amount of information in two clusterings relative to the information shared between them, thus providing a metric that decreases to 0 as the overlap between two partitions grows; see [49] for a discussion of the key properties of VI that facilitate uncertainty quantification on partitions. Under this framework, a formal Bayesian point estimate for \mathbf{z} is that partition with lowest posterior averaged VI distance from the other clusterings, thus obtaining

$$\hat{\mathbf{z}} = \arg \min_{\mathbf{z}'} \mathbb{E}_{\mathbf{z}'} [\text{VI}(\mathbf{z}, \mathbf{z}') \mid \mathbf{Y}], \quad (15)$$

where the expectation is taken with respect to \mathbf{z} . Due to the huge cardinality of the partition space, even for moderate V , the optimization in (15) is typically carried out through a greedy algorithm [49], as in the R package `mcclust.ext`.

The VI distance also provides natural strategies to construct credible sets around point estimates. In particular, one can define a $1 - \alpha$ credible ball around $\hat{\mathbf{z}}$ by ordering the partitions according to their VI distance from $\hat{\mathbf{z}}$, and defining the

ball as containing all the partitions having less than a threshold distance from $\hat{\mathbf{z}}$, with the threshold chosen to minimize the size of the ball while ensuring it contains at least $1 - \alpha$ posterior probability. Summarizing this ball is non-trivial given the high-dimensional discrete nature of the space of partitions. In practice, as we illustrate in our examples below, one can report the partition at the edge of the ball, which we call a credible bound. This form of uncertainty quantification complements the posterior *co-clustering matrix* which presents, for every pair of nodes, the relative frequency of MCMC samples in which such nodes are assigned to the same community.

Another advantage of a Bayesian approach over algorithmic techniques is the possibility of model selection through formal testing. In particular, we can test two models \mathcal{M} and \mathcal{M}' against each other by studying the Bayes factor [24]

$$\mathcal{B}_{\mathcal{M}, \mathcal{M}'} = \frac{p(\mathbf{Y} \mid \mathcal{M})}{p(\mathbf{Y} \mid \mathcal{M}')} = \frac{\sum_{\mathbf{z}} p(\mathbf{Y} \mid \mathbf{z}) p(\mathbf{z} \mid \mathcal{M})}{\sum_{\mathbf{z}} p(\mathbf{Y} \mid \mathbf{z}) p(\mathbf{z} \mid \mathcal{M}')}. \quad (16)$$

Due to the unified structure of ESBMs, such an approach is highly general and allows comparisons between any two models in the ESBM class covering, for example, representations relying on different priors for \mathbf{z} and formulations including or not node attributes. While for degenerate models, with $p(\mathbf{z} \mid \mathcal{M}) = \delta_{\mathbf{z}'}$, computing $p(\mathbf{Y} \mid \mathcal{M})$ reduces to evaluating (3) at a specific \mathbf{z}' [27], for non-degenerate models we must rely on posterior samples $\mathbf{z}^{(1)}, \dots, \mathbf{z}^{(T)}$ from $p(\mathbf{z} \mid \mathbf{Y}, \mathcal{M})$ to obtain an estimate of $p(\mathbf{Y} \mid \mathcal{M})$, for example through the harmonic mean [37, 44]

$$\hat{p}(\mathbf{Y} \mid \mathcal{M}) = [T^{-1} \sum_{t=1}^T p(\mathbf{Y} \mid \mathbf{z}^{(t)})^{-1}]^{-1}, \quad (17)$$

where $p(\mathbf{Y} \mid \mathbf{z}^{(t)})$ is the marginal likelihood in (3) at $\mathbf{z}^{(t)}$. We shall note that (17) may face instabilities and slow convergence to $p(\mathbf{Y} \mid \mathcal{M})$, thus motivating other estimators [14]. Such issues did not occur in our empirical studies and the results were always coherent with other model assessment measures. Hence, we maintain (17) for its simplicity. As a global measure of goodness-of-fit we also study the misclassification error when predicting each y_{vu} with $\hat{\theta}_{\hat{z}_v \hat{z}_u}$.

4. Simulation Studies

To assess ESBM performance and highlight benefits over algorithmic strategies [4], we consider two simulated networks of $V = 100$ nodes with various types of block structures, both sampled from a SBM with $\bar{H}_0 = 5$ communities and block probabilities either 0.7 or 0.3. As illustrated in Figure 2, the first network has equally-sized groups of 20 nodes each, displaying either community or core-periphery patterns, whereas the second has a cluster of size 40, one of size 30 and the remaining three of size 10, all characterized by classical community structures. State-of-the-art algorithmic strategies [4] applied to these two networks failed in recovering the true underlying blocks and showed a tendency to over-collapse different communities, due to their inability to incorporate unbalanced noisy partitions and behaviors beyond community patterns.

The above result motivates implementation of ESBMs, both with and without attributes coinciding with the true partition \mathbf{z}_0 . Within the Gibbs-type class, we test the four representative priors (DM, DP, PY and GN) for \mathbf{z} presented in Table 1. Their hyperparameters are set so that the prior mean for the number H of non-empty clusters is close to $10 > \bar{H}_0$ under all priors. In this way we can check whether our results are robust to hyperparameters settings. Specifically, we set $\alpha = 2.55$ for the DP, $\sigma = 0.575$ and $\alpha = -0.325$ for the PY, $\bar{H} = 50$ and $\beta = 3/50$ for the DM and $\gamma = 0.475$ for the GN. In implementing these models we consider the default setting $a = b = 1$ for the prior on the block probabilities and let $\alpha_1 = \dots = \alpha_C = 1$ when including node attributes. From Algorithm 1 we obtain 15000 samples for \mathbf{z} , after a conservative burn-in of 5000. In our experiments, inference was robust with respect to the initialization of \mathbf{z} , but starting with one community for each node provided the best mixing — when monitored on the chain of the likelihood in (3), evaluated at the MCMC samples of \mathbf{z} . The traceplots for such a chain suggested rapid convergence under

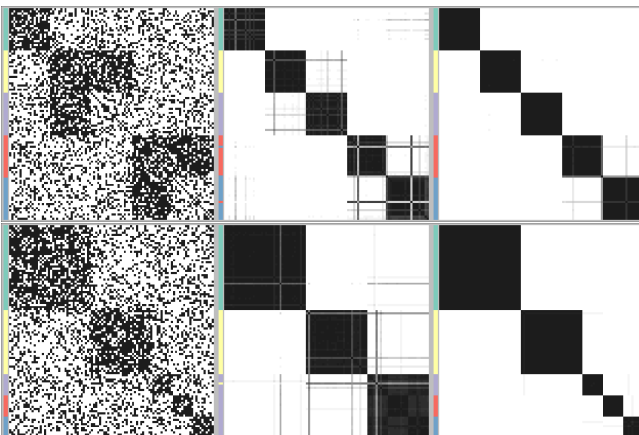


Figure 2. Left: observed adjacency matrix, with colors on the side corresponding to the true communities. Center and right: posterior co-clustering matrix under the Gnedin process from the ESBM without and with node attributes, respectively. Colors on the side correspond to the estimated partition. Top panel refers to the first simulated network, bottom panel to the second.

	$\log p(\mathbf{Y})$	$\mathbb{E}[\text{VI}(\mathbf{z}, \mathbf{z}_0) \mathbf{Y}]$	H	$\text{VI}(\hat{\mathbf{z}}, \mathbf{z}_0)$	$\text{VI}(\hat{\mathbf{z}}, \mathbf{z}_b)$
NETWORK 1 [WITHOUT ATTRIBUTES]					
DM	-3101.7	0.648	7 [6,8]	0.303	0.887
DP	-3101.6	0.631	7 [6,8]	0.303	0.860
PY	-3123.6	0.554	6 [6,7]	0.303	0.780
GN	-3097.5	0.519	5 [5,6]	0.303	0.724
NETWORK 1 [WITH ATTRIBUTES]					
DM	-3084.5	0.108	5 [5,6]	0.000	0.285
DP	-3083.7	0.105	5 [5,6]	0.000	0.265
PY	-3084.7	0.105	5 [5,6]	0.000	0.250
GN	-3083.3	0.085	5 [5,5]	0.000	0.230
NETWORK 2 [WITHOUT ATTRIBUTES]					
DM	-3148.4	0.837	6 [5,7]	0.570	1.009
DP	-3146.6	0.819	6 [5,7]	0.570	0.979
PY	-3145.3	0.762	4 [3,5]	0.570	0.776
GN	-3142.9	0.725	4 [3,5]	0.570	0.649
NETWORK 2 [WITH ATTRIBUTES]					
DM	-3123.7	0.052	5 [5,6]	0.000	0.189
DP	-3123.2	0.063	5 [5,6]	0.000	0.238
PY	-3124.0	0.081	5 [5,5]	0.000	0.285
GN	-3119.9	0.031	5 [5,5]	0.000	0.116

Table 2. Results of ESBMs in the two scenarios with $\bar{H}_0 = 5$ clusters.

Performance is measured by marginal likelihood $\log p(\mathbf{Y})$, posterior mean of the variation of information distance $\mathbb{E}[\text{VI}(\mathbf{z}, \mathbf{z}_0) | \mathbf{Y}]$ from the true partition \mathbf{z}_0 , the posterior median number of the non-empty clusters H (with first and third quartiles in brackets), distance $\text{VI}(\hat{\mathbf{z}}, \mathbf{z}_0)$ among the estimated and true partitions, and distance $\text{VI}(\hat{\mathbf{z}}, \mathbf{z}_b)$ among the estimated partition and the 95% credible bound.

all models, and Algorithm 1 provided 120 samples of \mathbf{z} per second when implemented on an iMac with 1 Intel Core i5 3.4 GHZ processor and 8 GB RAM, thus showing good efficiency. Table 2 summarizes the performance of the four priors, both with and without node attributes, in each of the two scenarios.

Among the four Gibbs-type priors considered for \mathbf{z} , the Gnedin process always performed slightly better in terms of marginal likelihood and posterior mean of the VI distance from the true partition \mathbf{z}_0 . More notably, it typically offered more accurate learning of the number of communities, with tighter interquartile ranges that always included the true $\bar{H}_0 = 5$, and tighter credible balls around the VI-optimal posterior point estimate $\hat{\mathbf{z}}$. The posterior bias in terms of VI distance between $\hat{\mathbf{z}}$ and true \mathbf{z}_0 is comparable under all four considered priors and much smaller than the maximum achievable VI among two partitions of 100 nodes, which is $\log_2 100 \approx 6.644$. In our trials, GN was also the most robust to hyperparameters.

As expected, including informative attributes improved performance, lowering by one order of magnitude the $\mathbb{E}[\text{VI}(\mathbf{z}, \mathbf{z}_0) | \mathbf{Y}]$, bringing $\text{VI}(\hat{\mathbf{z}}, \mathbf{z}_0)$ to zero and shrinking the credible balls. In a sense, this is the best scenario, since we used the true memberships \mathbf{z}_0 as attributes. We also tried supervising with a random permutation of \mathbf{z}_0 . This resulted in a slight performance deterioration relative to the model without attributes, which is doubly reassuring. In fact, on one hand it shows that the unsupervised model would be preferred to one with non-

informative attributes under the proposed model-selection criteria. On the other, the fact that performance deterioration is not dramatic suggests robustness in learning. According to Figure 2, unbalanced partitions are harder to infer, especially without attributes. However this gap vanishes when including informative attributes that can successfully support inference.

All misclassification errors were about 0.29, almost matching the one expected under the true model. This suggests accurate calibration and tendency to avoid overfitting in ESBMs.

5. Bill co-sponsorship networks

Motivated by the growing interest in the analysis of political networks [13, 6, 5, 46], we apply our proposed ESBM class to the bill co-sponsorship network among the $V = 655$ members of the Italian parliament during the 2013–2018 mandate, whose composition is reported in Table 3. This dataset is extracted from the more extensive openly-available data in [5], who provide legislative networks from 20 countries across years. Here, we consider the last available mandate of the Italian parliament and transform the original directed and weighted network into an undirected and binary one. Namely, we study the symmetric adjacency matrix \mathbf{Y} with elements $y_{vu} = y_{uv} = 1$ if v co-sponsored a bill authored by u or vice-versa, and $y_{vu} = y_{uv} = 0$ otherwise. The original edges were directed towards the first author of the bill and weighted in inverse proportion to the number of co-sponsors and total bills. However, for our purposes, such direction and weight seem less informative than the presence or absence of a co-sponsorship.

Given its appealing theoretical properties and in light of the results in simulations, we adopt a Gnedin process as a prior on \mathbf{z} within our ESBM formulation. The hyperparameter γ is set to 0.5, corresponding to 20 expected clusters a priori, twice as many as the parties in the legislature, which seems reasonably conservative. We run Algorithm 1 both with and without node attributes for 15000 iterations after a burn-in of 5000. Mixing was adequate as in the simulation, whereas the running times increased due to the much larger V , which requires one minute to produce 120 samples of \mathbf{z} . Despite

PARTY	SEATS	LEFT-RIGHT	WINGS
Sinistra Ecologia Libertà	34	1.3	LEFT
Movimento 5 Stelle	104	2.6	M5S
Partito Democratico	314	2.6	LEFT
Per l’Italia: Centro Democratico	11	6.0	LEFT
Scelta Civica per Monti	30	6.0	LEFT
Forza Italia (Il Popolo della Libertà)	72	7.1	RIGHT
Lega Nord	22	7.8	RIGHT
Alleanza Nazionale	9	8.1	RIGHT
Area Popolare	31	—	RIGHT
Mixed or minor group	28	—	MIXED

Table 3. Composition of the Italian parliament during the 2013–2018 mandate. For each party, we report the number of seats and the left-right score in [5], with 0 corresponding to extreme-left and 10 to extreme-right. The last column denotes the macro-alliances underlying the 2013–2018 legislature, that we use as attributes.

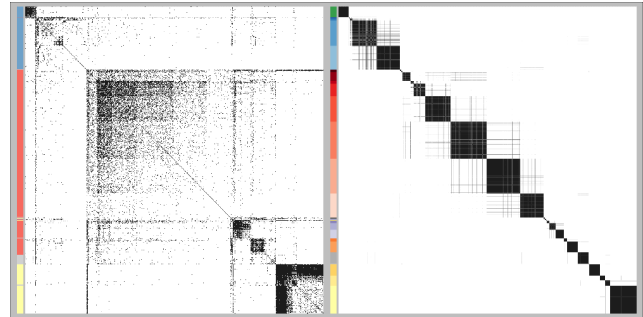


Figure 3. Left: observed bill co-sponsorship adjacency matrix, reordered according to the estimated communities; colors on the side correspond to political wings, used as node attributes: blue for the right wing, red for the left wing, yellow for *Movimento 5 Stelle* and grey for the mixed group. Right: posterior co-clustering matrix; colors on the side denote estimated clusters, with shades proportional to the prevailing party: green for *Lega Nord*, blue for the rest of the right wing, red for *Partito Democratico* and *Per l’Italia: Centro Democratico*, orange for *Scelta Civica per Monti*, purple for *Sinistra Ecologia Libertà*, yellow for *Movimento 5 stelle*, grey for the mixed group.

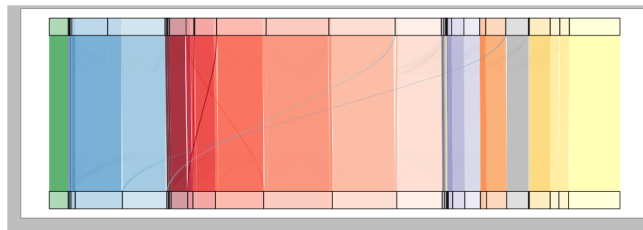


Figure 4. Riverplot highlighting which nodes change community when comparing the estimated partition $\hat{\mathbf{z}}$ with the bound \mathbf{z}_b of the 95% credible ball around $\hat{\mathbf{z}}$. Party colors are the same as in Figure 3.

this increment, running times under Algorithm 1 remain still feasible even for larger networks.

As shown in Table 3, node attributes are political wings denoting macro-alliances, which we found to be more informative than single parties, based on the marginal likelihood. As shown in Table 4, this measure suggests also a preference for the attribute-assisted model, meaning that such external groupings carry information about the block structures in the network. This is confirmed by the matrix in the left panel of Figure 3, in which, by reordering the nodes according to the inferred partition, we can observe a recurrent core-periphery pattern underlying each wing that was hidden in Figure 1 and could not have been captured by algorithmic approaches. This structure is suggestive of a system in which only a subset of politicians are active in proposing new bills, whereas the others are less active and tend to support just those bills proposed by members of the same wing. The right panel of Figure 3, instead, represents the posterior co-clustering matrix, which is quite sharp, suggesting limited posterior uncertainty. This is also highlighted by Figure 4 and is confirmed by the posterior summaries in Table 4. In fact, the radius of the credible ball is far below 1 under both models, while the maximum achievable VI distance is $\log_2 655 \approx 9.355$. The misclassification error of 0.05 confirms the satisfactory fit of the models.

The co-clustering matrix in Figure 3 also shows alliances among parties in the same wing and fragmentations within

	$\log p(\mathbf{Y})$	H	$\text{VI}(\hat{\mathbf{z}}, \mathbf{z}_b)$
WITHOUT ATTRIBUTES	-31835.06	32 [32,33]	0.540
WITH ATTRIBUTES [WINGS]	-31824.08	31 [31,31]	0.590

Table 4. Marginal likelihood $\log p(\mathbf{Y})$ and posterior summaries for the bill co-sponsorship network under the Gneden process: posterior median number of occupied communities H (with first and third quartiles in brackets) and distance $\text{VI}(\hat{\mathbf{z}}, \mathbf{z}_b)$ among the estimated partition $\hat{\mathbf{z}}$ and the 95% VI credible bound.

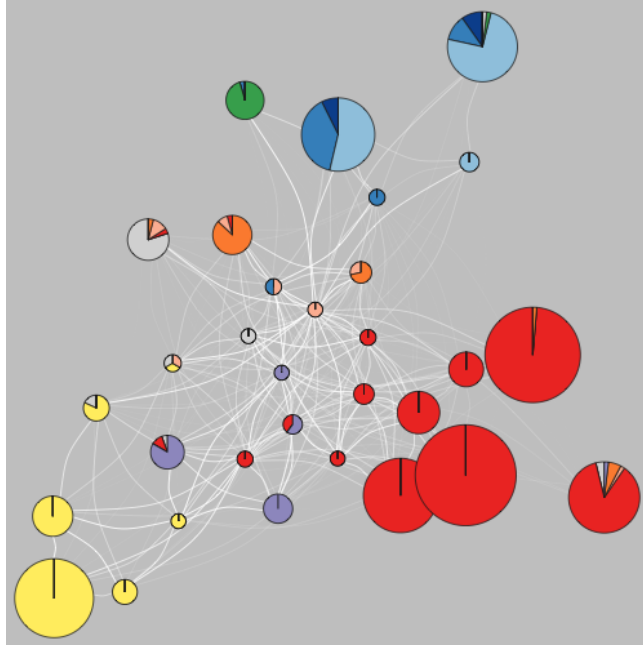


Figure 5. Network representation of inferred clusters. Each node denotes one community and edges are weighted by estimated block probabilities. Node sizes are proportional to cluster cardinalities, while pie-charts represent cluster compositions with respect to party affiliations (party colors are the same as in Figure 3). Node placement reflects the strength of connections (higher block probabilities result in closer nodes).

larger parties, mostly due to core–periphery structures. This can be observed also in Figure 5, where clusters are visualized as nodes of a new weighted network, with weights given by the block probabilities estimated via (14). Party memberships within each cluster are represented via pie–charts, thus highlighting different fragmentation and aggregation levels for the different parties. For example, all members of *Lega Nord* belong to the same community, while *Movimento 5 Stelle* and *Partito Democratico* are split over several blocks. Right-wing parties, instead, belong to two main communities with different party proportions. The “geography” of such communities, induced by the block probabilities, mostly reflects the left–right placement of Italian parties in Table 3, and highlights a polarization around three main forces, covering left parties, right parties and *Movimento 5 Stelle*, that are almost equidistant.

6. Discussion

In the present paper we have proposed ESBMs, a broad class of models that unifies most existing SBMs via Gibbs–type

priors. Besides providing a single methodological, theoretical and computational framework for various SBMs, such a generalization facilitates the proposal of new models by exploring alternative options within the Gibbs–type class, and allows natural inclusion of attributes via connections with PPMs. For example, we have shown in simulations that the Gneden process, which to the best of our knowledge had never been used in SBMs, can improve performance of the already–implemented DP, PY and DM. The illustrative political application outlines the benefits of our extended class of models and inference methods, capturing hidden block structures and core–periphery patterns.

The present work offers many directions for future research. For example, the highly modular structure of ESBMs facilitates extensions to directed, bipartite and weighted networks, as done by [45] for the infinite relational model. To address this goal, it is sufficient to substitute the beta–binomial likelihood in (3) with suitable ones, for example gamma–Poisson for count edges and Gaussian–Gaussian for continuous ones. Also other types of attributes beyond categorial ones can be easily included leveraging the default choices suggested by [33] for $p(\cdot)$ in (7) under continuous, ordinal and count–type attributes. Further extensions to other representations, such as the mixed membership SBM [1], and the development of more scalable algorithms are also worth being explored.

Acknowledgments

This work was partially supported by the PRIN–MIUR 2017 project 20177BRJXS and by grant R01ES027498 of the National Institute of Environmental Health Sciences of the United States National Institutes of Health.

References

- [1] AIROLDI, E. M., BLEI, D. M., FIENBERG, S. E., AND XING, E. P. Mixed membership stochastic blockmodels. *Journal of Machine Learning Research* 9 (2008), 1981–2014.
- [2] ATHREYA, A., FISHKIND, D. E., TANG, M., PRIEBE, C. E., PARK, Y., VOGELSTEIN, J. T., LEVIN, K., LYZINSKI, V., AND QIN, Y. Statistical inference on random dot product graphs: a survey. *Journal of Machine Learning Research* 18 (2017), 8393–8484.
- [3] BICKEL, P., CHOI, D., CHANG, X., ZHANG, H., ET AL. Asymptotic normality of maximum likelihood and its variational approximation for stochastic blockmodels. *Annals of Statistics* 41 (2013), 1922–1943.

- [4] BLONDEL, V. D., GUILLAUME, J. L., LAMBIOTTE, R., AND LEFEBVRE, E. Fast unfolding of communities in large networks. *Journal of Statistical Mechanics* 10 (2008), P10008.
- [5] BRIATTE, F. Network patterns of legislative collaboration in twenty parliaments. *Network Science* 4 (2016), 266–271.
- [6] CRANMER, S. J., AND DESMARAIS, B. A. Inferential network analysis with exponential random graph models. *Political analysis* 19 (2011), 66–86.
- [7] CROSSLEY, N. A., MECELLI, A., VÉRTES, P. E., WINTON-BROWN, T. T., PATEL, A. X., GINESTET, C. E., MCGUIRE, P., AND BULLMORE, E. T. Cognitive relevance of the community structure of the human brain functional coactivation network. *Proceedings of the National Academy of Sciences* 110 (2013), 11583–11588.
- [8] DE BLASI, P., FAVARO, S., LIJOI, A., MENA, R. H., PRÜNSTER, I., AND RUGGIERO, M. Are Gibbs-type priors the most natural generalization of the Dirichlet process? *IEEE Transactions on Pattern Analysis and Machine Intelligence* 37 (2013), 212–229.
- [9] DE BLASI, P., LIJOI, A., AND PRÜNSTER, I. An asymptotic analysis of a class of discrete nonparametric priors. *Statistica Sinica* 23, 3 (2013), 1299–1321.
- [10] FORTUNATO, S. Community detection in graphs. *Physics Reports* 486 (2010), 75–174.
- [11] FORTUNATO, S., AND HRIC, D. Community detection in networks: A user guide. *Physics Reports* 659 (2016), 1–44.
- [12] FOSDICK, B. K., MCCORMICK, T. H., MURPHY, T. B., NG, T. L. J., AND WESTLING, T. Multiresolution network models. *Journal of Computational and Graphical Statistics* 28 (2019), 185–196.
- [13] FOWLER, J. H. Connecting the congress: A study of cosponsorship networks. *Political Analysis* 14 (2006), 456–487.
- [14] GELMAN, A., AND MENG, X.-L. Simulating normalizing constants: from importance sampling to bridge sampling to path sampling. *Statistical Science* 13, 2 (1998), 163–185.
- [15] GENG, J., BHATTACHARYA, A., AND PATI, D. Probabilistic community detection with unknown number of communities. *Journal of the American Statistical Association* 114 (2019), 893–905.
- [16] GIRVAN, M., AND NEWMAN, M. E. Community structure in social and biological networks. *Proceedings of the National Academy of Sciences* 99 (2002), 7821–7826.
- [17] GNEDIN, A. Species sampling model with finitely many types. *Electronic Communications in Probability* 15 (2010), 79–88.
- [18] GNEDIN, A., AND PITMAN, J. Exchangeable Gibbs partitions and Stirling triangles. *Zapiski Nauchnykh Seminarov, POMI* 325 (2005), 83–102.
- [19] GUIMERA, R., MOSSA, S., TURTSCHI, A., AND AMARAL, L. N. The worldwide air transportation network: Anomalous centrality, community structure, and cities' global roles. *Proceedings of the National Academy of Sciences* 102 (2005), 7794–7799.
- [20] HANDCOCK, M. S., RAFTERY, A. E., AND TANTRUM, J. M. Model-based clustering for social networks. *Journal of the Royal Statistical Society: Series A* 170 (2007), 301–354.
- [21] HARTIGAN, J. Partition models. *Communications in Statistics - Theory and Methods* 19 (1990), 2745–2756.
- [22] HOLLAND, P. W., LASKEY, K. B., AND LEINHARDT, S. Stochastic blockmodels: First steps. *Social Networks* 5 (1983), 109–137.
- [23] KARRER, B., AND NEWMAN, M. E. Stochastic blockmodels and community structure in networks. *Physical Review E* 83 (2011), 016107.
- [24] KASS, R. E., AND RAFTERY, A. E. Bayes factors. *Journal of the American Statistical Association* 90 (1995), 773–795.
- [25] KEMP, C., TENENBAUM, J. B., GRIFFITHS, T. L., YAMADA, T., AND UEDA, N. Learning systems of concepts with an infinite relational model. In *Proceedings of the 21st National Conference on Artificial Intelligence - Volume 1* (2006), pp. 381–388.
- [26] LEE, C., AND WILKINSON, D. J. A review of stochastic block models and extensions for graph clustering. *Applied Network Science* 4 (2019), 1–50.
- [27] LEGRAMANTI, S., RIGON, T., AND DURANTE, D. Bayesian testing for exogenous partition structures in stochastic block models. *Manuscript Submitted for Publication* (2020).
- [28] LIJOI, A., MENA, R. H., AND PRÜNSTER, I. Controlling the reinforcement in Bayesian non-parametric mixture models. *Journal of the Royal Statistical Society. Series B* 69, 4 (2007), 715–740.
- [29] LIU, F., CHOI, D., XIE, L., AND ROEDER, K. Global spectral clustering in dynamic networks. *Proceedings of the National Academy of Sciences* 115 (2018), 927–932.
- [30] MEILĀ, M. Comparing clusterings — an information based distance. *Journal of Multivariate Analysis* 98, 5 (2007), 873–895.
- [31] MILLER, J. W., AND HARRISON, M. T. Inconsistency of Pitman-Yor process mixtures for the number of components. *Journal of Machine Learning Research* 15, 1 (2014), 3333–3370.
- [32] MILLER, J. W., AND HARRISON, M. T. Mixture models with a prior on the number of components. *Journal of the American Statistical Association* 113 (2018), 340–356.

[33] MÜLLER, P., QUINTANA, F., AND ROSNER, G. L. A product partition model with regression on covariates. *Journal of Computational and Graphical Statistics* 20, 1 (2011), 260–278.

[34] NEWMAN, M. E. Modularity and community structure in networks. *Proceedings of the National Academy of Sciences* 103 (2006), 8577–8582.

[35] NEWMAN, M. E., AND CLAUSET, A. Structure and inference in annotated networks. *Nature Communications* 7 (2016), 1–11.

[36] NEWMAN, M. E. J., AND GIRVAN, M. Finding and evaluating community structure in networks. *Physical Review E* 69 (2004), 026113.

[37] NEWTON, M. A., AND RAFTERY, A. E. Approximate Bayesian inference with the weighted likelihood bootstrap. *Journal of the Royal Statistical Society. Series B* 56 (1994), 3–26.

[38] NOWICKI, K., AND SNIJDERS, T. A. B. Estimation and prediction for stochastic blockstructures. *Journal of the American Statistical Association* 96 (2001), 1077–1087.

[39] OLHEDE, S. C., AND WOLFE, P. J. Network histograms and universality of blockmodel approximation. *Proceedings of the National Academy of Sciences* 111 (2014), 14722–14727.

[40] PARK, A. J.-H., AND DUNSON, D. B. Bayesian generalized product partition model. *Statistica Sinica* 20, 3 (2010), 1203–1226.

[41] PITMAN, J. Some developments of the Blackwell-MacQueen urn scheme. *Statistics, Probability and Game Theory* 30 (1996), 245–267.

[42] PRIEBE, C. E., PARK, Y., VOGELSTEIN, J. T., CONROY, J. M., LYZINSKI, V., TANG, M., ATHREYA, A., CAPE, J., AND BRIDGEFORD, E. On a two-truths phenomenon in spectral graph clustering. *Proceedings of the National Academy of Sciences* 116 (2019), 5995–6000.

[43] QUINTANA, F. A., AND IGLESIAS, P. L. Bayesian clustering and product partition models. *Journal of the Royal Statistical Society. Series B* 65, 2 (2003), 557–574.

[44] RAFTERY, A. E., NEWTON, M. A., SATAGOPAN, J. M., AND KRIVITSKY, P. N. Estimating the integrated likelihood via posterior simulation using the harmonic mean identity. *Bayesian Statistics* 8 (2007), 1–45.

[45] SCHMIDT, M. N., AND MORUP, M. Nonparametric Bayesian modeling of complex networks: An introduction. *IEEE Signal Processing Magazine* 30 (2013), 110–128.

[46] SIGNORELLI, M., AND WIT, E. C. A penalized inference approach to stochastic block modelling of community structure in the italian parliament. *Journal of the Royal Statistical Society: Series C* 67 (2018), 355–369.

[47] STANLEY, N., BONACCI, T., KWITT, R., NIETHAMMER, M., AND MUCHA, P. J. Stochastic block models with multiple continuous attributes. *Applied Network Science* 4 (2019), 1–22.

[48] TALLBERG, C. A Bayesian approach to modeling stochastic blockstructures with covariates. *Journal of Mathematical Sociology* 29 (2004), 1–23.

[49] WADE, S., AND GHAHRAMANI, Z. Bayesian cluster analysis: Point estimation and credible balls. *Bayesian Analysis* 13 (2018), 559–626.

[50] ZHAO, Y., LEVINA, E., AND ZHU, J. Community extraction for social networks. *Proceedings of the National Academy of Sciences* 108 (2011), 7321–7326.

[51] ZHAO, Y., LEVINA, E., AND ZHU, J. Consistency of community detection in networks under degree-corrected stochastic block models. *Annals of Statistics* 40 (2012), 2266–2292.